Chimeric siRNAs with chemically modified pentofuranose and hexopyranose nucleotides: altritol-nucleotide (ANA) containing GalNAc–siRNA conjugates: *in vitro* and *in vivo* RNAi activity and resistance to 5′-exonuclease

Pawan Kumar[1], Rohan Degaonkar[1], Dale C. Guenther[1], Mikhail Abramov[2], Guy Schepers[2], Marie Capobianco[1], Yongfeng Jiang[1], Joel Harp[3], Charalambos Kaittanis[1], Maja M. Janas[1], Adam Castoreno[1], Ivan Zlatev[1], Mark K. Schlegel[1], Piet Herdewijn [ID][2], Martin Egli [ID][3] and Muthiah Manoharan [ID][1],*

[1]Alnylam Pharmaceuticals, 300 Third Street, Cambridge, MA 02142, USA, [2]Medicinal Chemistry, Rega Institute for Medical Research, KU Leuven, Herestraat 49, 3000 Leuven, Belgium and [3]Department of Biochemistry, School of Medicine, Vanderbilt University, Nashville, TN 37232, USA

ABSTRACT

In this report, we investigated the hexopyranose chemical modification Altriol Nucleic Acid (ANA) within small interfering RNA (siRNA) duplexes that were otherwise fully modified with the 2′-deoxy-2′-fluoro and 2′-*O*-methyl pentofuranose chemical modifications. The siRNAs were designed to silence the transthyretin (*Ttr*) gene and were conjugated to a trivalent *N*-acetylgalactosamine (GalNAc) ligand for targeted delivery to hepatocytes. Sense and antisense strands of the parent duplex were synthesized with single ANA residues at each position on the strand, and the resulting siRNAs were evaluated for their ability to inhibit *Ttr* mRNA expression *in vitro*. Although ANA residues were detrimental at the 5′ end of the antisense strand, the siRNAs with ANA at position 6 or 7 in the seed region had activity comparable to the parent. The siRNA with ANA at position 7 in the seed region was active in a mouse model. An Oligonucleotide with ANA at the 5′ end was more stable in the presence of 5′-exonuclease than an oligonucleotide of the same sequence and chemical composition without the ANA modification. Modeling studies provide insight into the origins of regiospecific changes in potency of siRNAs and the increased protection against 5′-exonuclease degradation afforded by the ANA modification.

INTRODUCTION

The tremendous potential of small interfering RNAs (siRNAs) in the development of new medicines is demonstrated by the success of patisiran (ONPATTRO®), a first in class drug for the treatment of hereditary transthyretin-mediated amyloidosis and the recent approval (https://www.givlaari.com, https://www.fda.gov/drugs/resources-information-approved-drugs/fda-approves-givosiran-acute-hepatic-porphyria, https://www.fda.gov/news-events/press-announcements/fda-approves-first-treatment-inherited-rare-disease) of the second compound givosiran (GIVLAARI™ for the treatment of acute hepatic porphyria (AHP) (1–6). Many other siRNAs are being evaluated in early to late stage clinical trials (7). siRNAs act through a natural gene regulatory mechanism called RNA interference (RNAi) to silence the expression of a targeted gene (8,9). siRNAs composed of natural RNA nucleotides are rapidly degraded and do not readily reach their target organ when administered systemically. Thus, it is necessary to use chemically modified siRNAs for therapeutic applications (10–14). Typically, siRNAs are modified using terminal phosphorothioate backbone linkages and 2′-deoxy-2′-fluoro (2′-F) (15–21) and 2′-*O*-methyl (2′-*O*Me) nucleotide modifications (Figure 1A and B) to increase metabolic stability. Conjugation to a trivalent *N*-acetylgalactosamine (GalNAc, Figure 1C) ligand, one that allows for the specific recognition and uptake by the asialoglycoprotein receptor (ASGPR) expressed on the surface of hepatocytes, results in targeting to the liver (22). We are investigating additional chemically modified
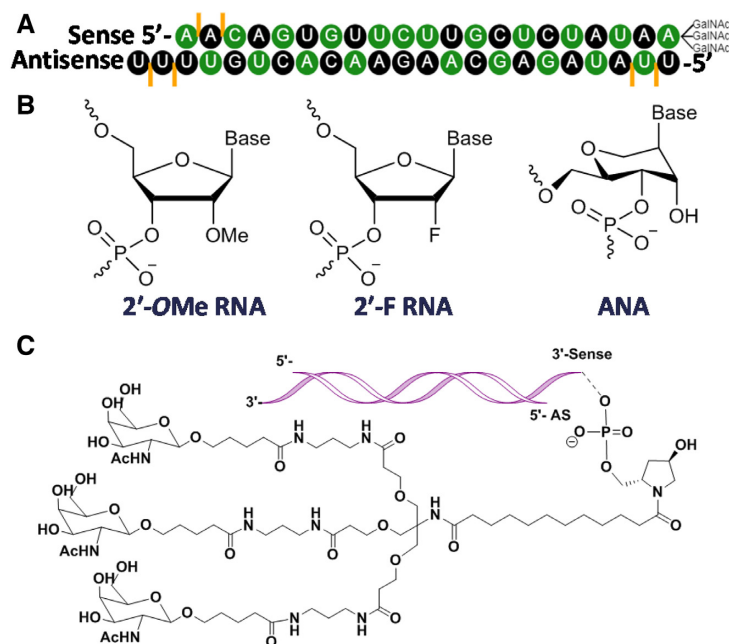

Figure 1. (**A**) Parent duplex targeting Ttr mRNA (14,25). Black circles represent 2′-OMe RNA, green circles represent 2′-F RNA, and orange vertical bars represent PS backbone modification sites. (**B**) Structures of 2′-OMe RNA, 2′-F RNA and ANA nucleotides. (**C**) Structure of a ternary GalNAc moiety attached to the 3′-end of an siRNA (shown as a ribbon).

nucleotides that can be used in synergy with 2′-F RNA and 2′-OMe RNA for generating potent and safe siRNAs (23–26). For instance, modification of the seed region of the antisense strand with glycol nucleic acid (GNA) can reduce seed-mediated off-target effects (24,27–32). Similarly, placing a 5′-morpholino-2′-OMe RNA nucleotide on the sense strand or a 5′-trans-vinylphosphonate-2′-OMe RNA nucleotide on the antisense strand can improve RNAi activity and specificity (23,33–39). Moreover, incorporation of 4′-C-methoxy-2′-deoxy-2′-fluoro uridine improves metabolic stability without reducing gene silencing activity (26).

Altritol nucleic acids (ANA) have a six-membered sugar with a nucleobase at the 2′-(S)-position and a hydroxyl group at the 3′-position (Figure 1B) (40,41). ANA has a pre-organized structure similar to the conformation of an N-type furanose sugar, and the presence of the hydroxyl group at the 3′-position contributes to duplex stabilization via hydration (40). The RNA-like A-type geometry of ANA makes it a candidate for incorporation into siRNAs, as this feature is important for RISC loading. ANA-modified siRNAs have been evaluated and were demonstrated to have some promise; (28,42–44) however, the ANA modification has not been tested in the context of other modified nucleotides or in siRNAs conjugated to ligands. More importantly, ANA modified siRNAs have never been tested *in vivo*. Here we evaluated the *in vitro* and *in vivo* gene silencing activity of siRNA duplexes modified with ANA, 2′-F RNA and 2′-OMe RNA nucleotides and conjugated to a trivalent GalNAc moiety (Figure 1A) (14,25). We also evaluated how effectively terminal ANA residues protected the oligonucleotides against nucleolytic degradation. siRNAs modified at single positions were as active as the parent

siRNA in RNAi-mediated gene-silencing. Furthermore, it is interesting that two terminal ANA residues imparted resistance to phosphodiesterase II, a 5′-exonuclease. Models of an siRNA guide strand with an ANA modification at position 7 bound to Argonaute 2 (Ago2) and an RNA with two 5′-terminal ANA residues bound to Xrn1, an RNA 5′-exonuclease helped rationalize the favorable RNAi pharmacological activity and metabolic stability, respectively.

MATERIALS AND METHODS

Oligonucleotide synthesis

ANA-modified oligonucleotides were synthesized following the previously published protocol (25) with the exception that 3% trichloroacetic acid in CH_2Cl_2 was used for detritylation.

In vitro siRNA activity analyses

First, 5 μl of siRNA was placed in each well of a 384-well collagen-coated plate, followed by addition of 4.90 μl of Opti-MEM and 0.1 μl of Lipofectamine RNAiMax (Invitrogen) to each well. Each siRNA was assessed in quadruplicate at final concentrations of 0.1 or 10 nM. Plates were incubated at room temperature for 15 min. Primary mouse hepatocyte cells were suspended in Invitrogro CP rodent medium (BioIVT, #Z990028), and 40 μl of this suspension (containing ∼5000 cells) was added to each well. After incubating the cells for 24 h, RNA was isolated using DynaBeads (ThermoFisher). The RNA was then reverse transcribed into cDNA according to the manufacturer's protocol (Applied Biosystems). Multiplex quantitative polymerase chain reaction (qPCR) reactions were per-

formed using a gene-specific TaqMan assay for *Ttr* (ThermoFisher Scientific, # Mm00443267_m1) and mouse *Gapdh* (#4352339E) as an endogenous control. Real-time PCR was performed on a Roche LightCycler 480 using LightCycler 480 Probes Master Mix (Roche). The details of the *in vitro* analysis has been described in detail in the references 25, 53, 54 and 55: the siRNA concentration required to inhibit relative TTR expression by 50% (IC_{50}) was calculated for a subset of the siRNAs by transfecting as described, eight concentrations ranging from 10 nM to 37.5 fM in a 6-fold dilution series. IC_{50} values were derived from a four parameter fit model with XLFit.

Off-target assay

COS-7 cells were cultured at 37°C, 5% CO_2 in Dulbecco's-modified eagle medium supplemented with 10% fetal bovine serum. Cells were co-transfected in 96-well plates (15 000 cells/well) with 10 ng luciferase reporter plasmid and 0.64 pM to 50 nM siRNA in 5-fold dilutions using 2 μg/ml Lipofectamine 2000 (Thermo Fisher Scientific) according to the manufacturer's instructions. Cells were harvested 48 h after transfection for the dual luciferase assay (Promega) performed according to the manufacturer's instructions. The on-target reporter plasmid contained a single perfectly complementary site (5′-AAAACAGTGTTCTTGCTCTATAA-3′) to the antisense strand of the *Ttr* siRNA in the 3′-untranslated (3′ UTR) of *Renilla* luciferase. The off-target reporter plasmid contained four tandem seed-complementary sites (5′-GCTCTATAA) separated by a 19-nucleotide spacer (5′-TAATATTACATAAATAAAA-3′) in the 3′-UTR of *Renilla* luciferase (27,29–30,45–46). Both plasmids co-expressed firefly luciferase as a transfection control.

In vivo gene expression silencing

All studies were conducted using protocols consistent with local, state and federal regulations, as applicable, and were approved by the Institutional Animal Care and Use Committee (IACUC) at Alnylam Pharmaceuticals. Female C56BL/6 mice (Charles River Laboratories) of 6–8 weeks old were dosed subcutaneously with 1 mg/kg siRNA formulated in 200 μl 1 × phosphate-buffered saline (PBS); the control cohort received the same volume of 1 × PBS. Since Ttr bound to pre-albumin can be found in circulation, blood samples were collected just prior to treatment administration and 7 and 14 days after siRNA dosing. The collected serum samples were stored at −80°C until analysis. Two weeks after compound administration, the animals were euthanized and livers were harvested and cryopreserved. Isolation of RNA from liver was done with the PerkinElmer Chemagic system according to the supplier's guidelines, then cDNA was prepared and multiplexed RT-qPCR analysis was performed to assess *Ttr* transcript levels using Taqman probe Mm00443267_m1 (ABI). *Gapdh* was quantified as a control (Taqman probe 4351309, ABI). Quantification of the TTR protein levels in serum was done spectrophotometrically with a mouse pre-albumin/TTR ELISA kit (41-PALMS-E01, ALPCO), in accordance to the manufacturer's protocol.

Nuclease stability assay

To assess stability in the presence of 3′- or 5′-specific exonucleases, modified oligonucleotides were prepared in a final concentration of 0.1 mg/ml in either 50 mM Tris (pH 7.2) with 10 mM $MgCl_2$ or 50 mM sodium acetate (pH 6.5) with 10 mM $MgCl_2$, respectively. The exonuclease (150 mU/ml SVPDE or 500 mU/ml phosphodiesterase II) was added just prior to analysis. Samples were analyzed using IEX HPLC (Dionex DNAPac PA200, 4 × 250 mm) using a gradient of 37–52% (mobile phase A: 20 mM sodium phosphate, 15% CH_3CN, pH 11; mobile phase B: 1 M NaBr, 20 mM sodium phosphate, pH 11, 15% CH_3CN) over 7.5 min with a flow of 1 ml/min. The amount of full-length oligonucleotide was determined as the area under the curve at A_{260}. The percent full-length oligonucleotide was calculated by dividing by the area under the curve at $t = 0$ and multiplying by 100. The activity of enzyme was compared to 5′-$(dT_{19})U_sU$-3′ or 5′-$U_sU(dT_{19})$-3′ for 3′- or 5′-exonuclease activity, respectively. In these sequences, the 's' indicates a phosphorothioate linkage; the other linkages were phosphodiester. Each aliquot of stock enzyme was thawed just prior to the experiment. The half-life was determined by fitting to first order kinetics.

Molecular modeling

Coordinates of the crystal structure of the ANA:RNA hybrid duplex (ANA strand: 5′-P-CCGUAAUGCC-3′, where P is a phosphate; RNA strand: 5′-GGCAUUACGG-3′) with PDB ID: 3OK2 (47) and the crystal structure of micro-RNA miR-20a bound to human Argonaute 2 (Ago2) with PDB ID: 4F3T (48) were retrieved from the Protein Data Bank www.rcsb.org. The G residue at position 7 of the RNA in the Ago2 complex was excised and replaced by ANA-G3 from the hybrid duplex with the ANA A-strand using the program UCSF Chimera (49). The geometry of the resulting fusion model was locally refined with Amber14 (50), and the glycosidic torsion angle of the ANA purine residue was adjusted slightly to restore stacking on the adjacent residue C8 as seen in the crystal structure of the Ago2 complex with native RNA.

Coordinates of the crystal structure of the complex between the *Drosophila melanogaster* Xrn1 5′-exoribonuclease and 5′P-dTdTdT-3′ with PDB ID: 2Y35 (51) were obtained from the Protein Data Bank. The ANA dimer at positions 9 and 10 was excised from strand A of the crystal structure of the ANA:RNA hybrid duplex and the bases converted to U using the program UCSF Chimera. The dimer was then superimposed on the first two nucleotides from the dT trimer in the Xrn1 complex with the match function in UCSF Chimera using selected backbone and base atoms.

Coordinates of the crystal structure of the complex between the *Escherichia coli* DNA polymerase I Klenow fragment 3′-exonuclease and 3′-dGdCdA-P5′ with PDB ID: 1KFS (52) were obtained from the Protein Data Bank. The ANA CG dimer (positions 2 and 3) was excised from strand A of the crystal structure of the ANA:RNA hybrid duplex and the dimer then superimposed on the d(CG) dimer in the Klenow exo complex with the match func-
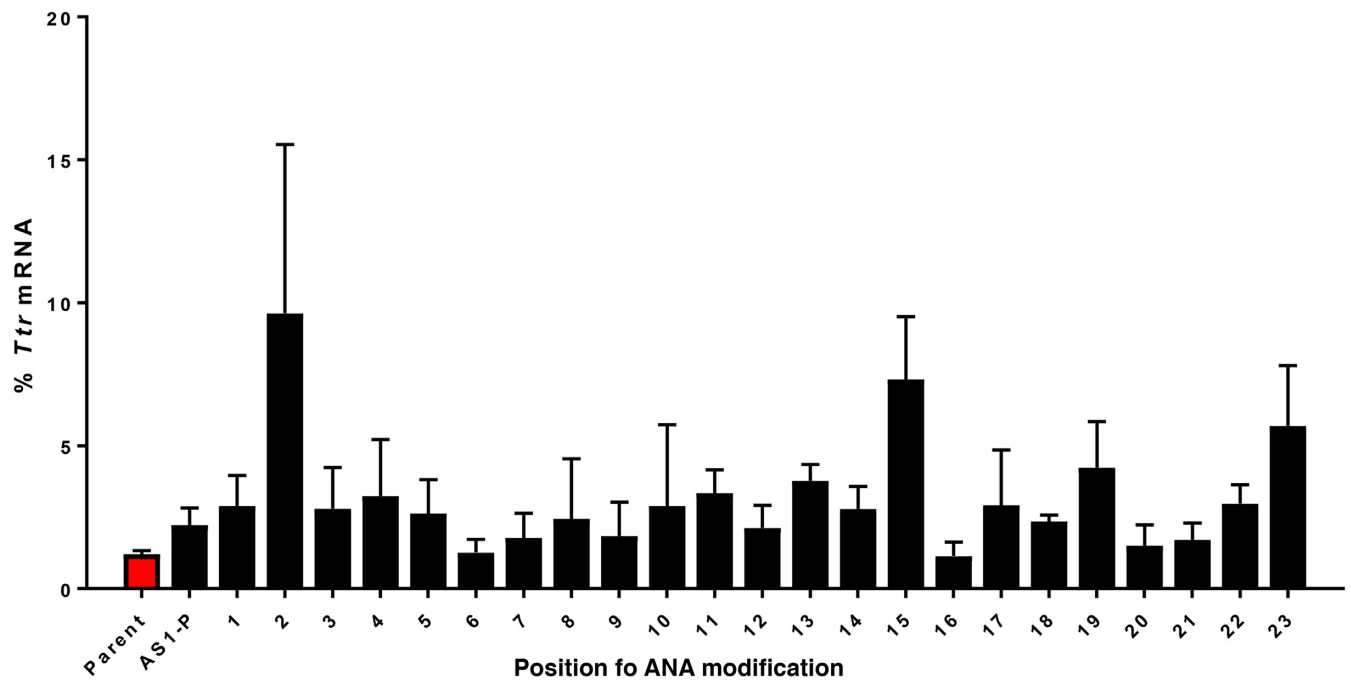
Figure 2. *In vitro* RNAi activity of siRNAs with ANA in the antisense strand in the presence of a transfecting agent. The nucleotide at the position indicated on the x-axis was substituted with the corresponding ANA nucleotide. siRNAs were tested at a concentration of 10 nM in primary mouse hepatocytes. Plotted is the % *Ttr* mRNA remaining relative to untreated cells ($n = 4$, mean ± SD).
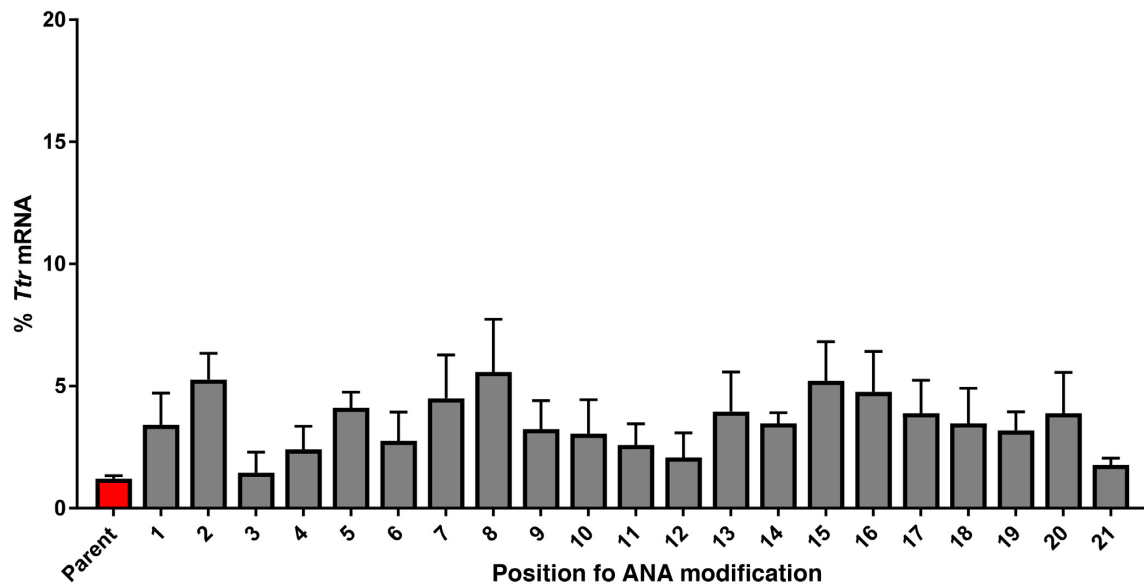

Figure 3. *In vitro* RNAi activity of siRNAs with ANA in the sense strand in the presence of a transfecting agent. The nucleotide at the position indicated on the x-axis was substituted with the corresponding ANA nucleotide. siRNAs were tested at a concentration of 10 nM in primary mouse hepatocytes. Plotted is the % *Ttr* mRNA remaining relative to untreated cells ($n = 4$, mean ± SD).

tion in UCSF Chimera using selected backbone and base atoms. In Chimera, 2′-hydroxyl groups were attached to 2′-deoxyribonucleases of the d(CG) dimer to generate a model of the Klenow exo complex with RNA bound. Next, coordinates of the ANA and RNA model complexes were stored and separately refined with Amber 14 in the Chimera suite using both steepest descent and con-

jugate gradient cycles until convergence, i.e. no further change in distances between RNA/ANA 2′-OH groups and atoms from Klenow exo side chains (Tyr-423 Cδ2/Thr-358 Oγ) and main chain (Thr-358 O). At last, all three complexes (DNA, RNA, ANA) were overlaid in UCSF Chimera using only Klenow fragment atoms with the match option.
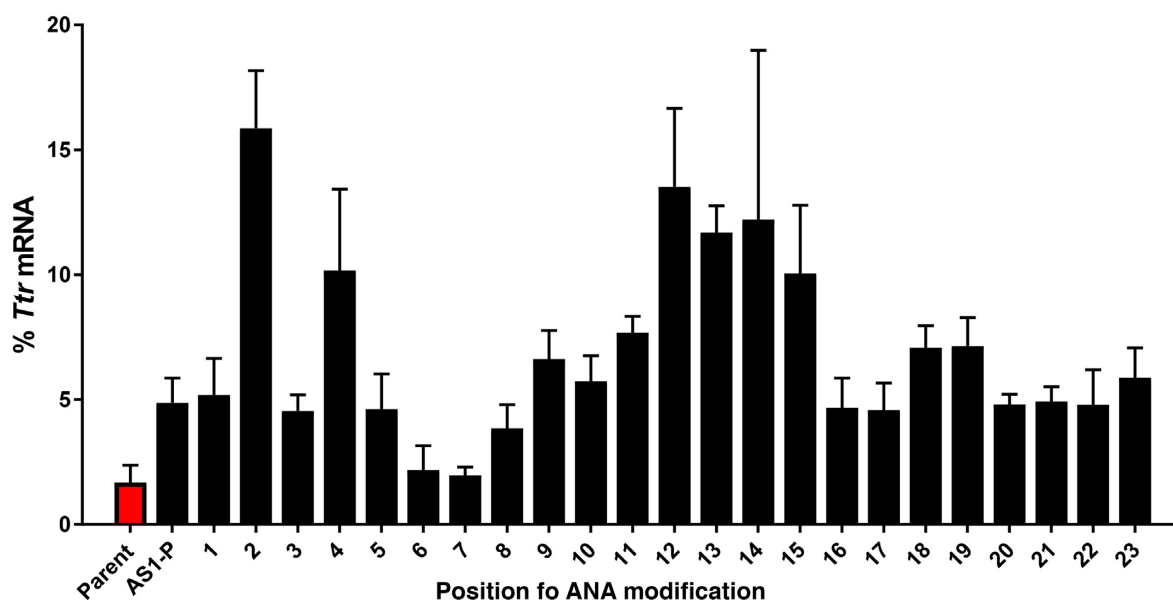
Figure 4. *In vitro* RNAi activity of siRNAs with ANA in the antisense strand in the absence of a transfecting agent (free uptake). The nucleotide at the position indicated on the x-axis was substituted with the corresponding ANA nucleotide. siRNAs were tested at a concentration of 100 nM in primary mouse hepatocytes. Plotted is the % *Ttr* mRNA remaining relative to untreated cells ($n = 4$, mean $\pm$ SD).
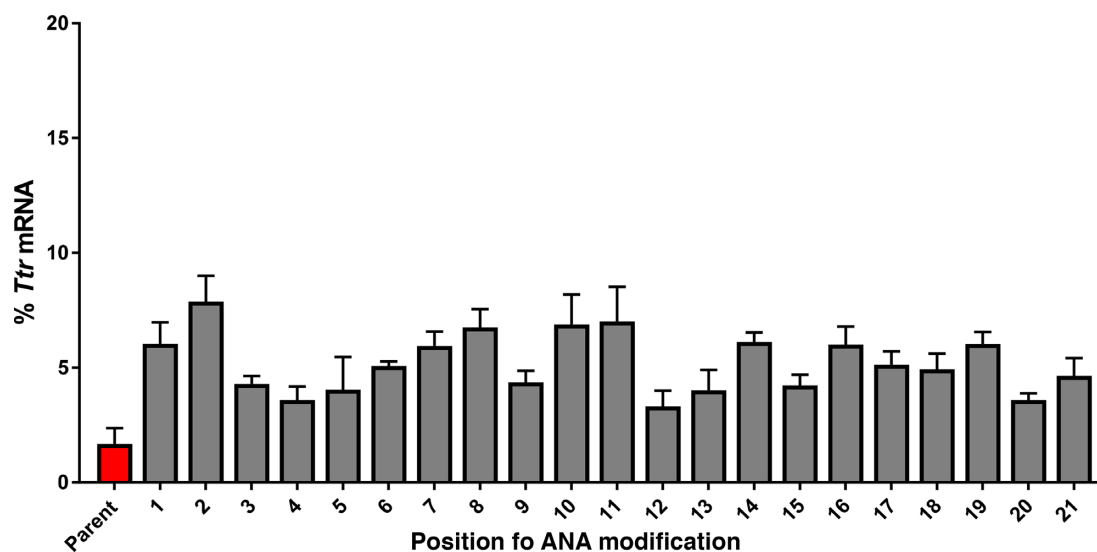

Figure 5. *In vitro* RNAi activity of siRNAs with ANA in the sense strand in the absence of a transfecting agent (free uptake). The nucleotide at the position indicated on the x-axis was substituted with the corresponding ANA nucleotide. siRNAs were tested at a concentration of 100 nM in primary mouse hepatocytes. Plotted is the % *Ttr* mRNA remaining relative to untreated cells ($n = 4$, mean $\pm$ SD).

RESULTS

In vitro activity of ANA-modified siRNAs

The position-dependent impact of the ANA modification on *in vitro* RNAi activity was assessed by systematically replacing each nucleotide of a previously studied siRNA designed to target rodent (mouse and rat) transthyretin (*Ttr*) mRNA (Figure 1) with an ANA residue (25,53–55). The parent siRNA is a 21-mer duplex with a two-nucleotide single-overhang on the 3′-end antisense strand modified with 2′-F RNA and 2′-*O*Me RNA nucleotides and is adapted from our earlier studies (14,25). The ends were

protected by introducing two phosphorothioate linkages at each strand extremity, except for the 3′-end of the sense strand, which is conjugated to a trivalent GalNAc ligand for targeted delivery to the liver (Figure 1A) (14,25). The RNAi activity of the resulting siRNAs with single ANA residues was studied in primary mouse hepatocytes (Figure 2). In agreement with a previous study, ANA at the 5′-end of the antisense strand (Figure 2, AS1) reduced potency (42). This loss in activity is probably due to the inability of cellular kinases to introduce a 5′-monophosphate group on the ANA nucleotide. The 5′-monophosphate plays an important role in RISC loading by interacting with the Ago2
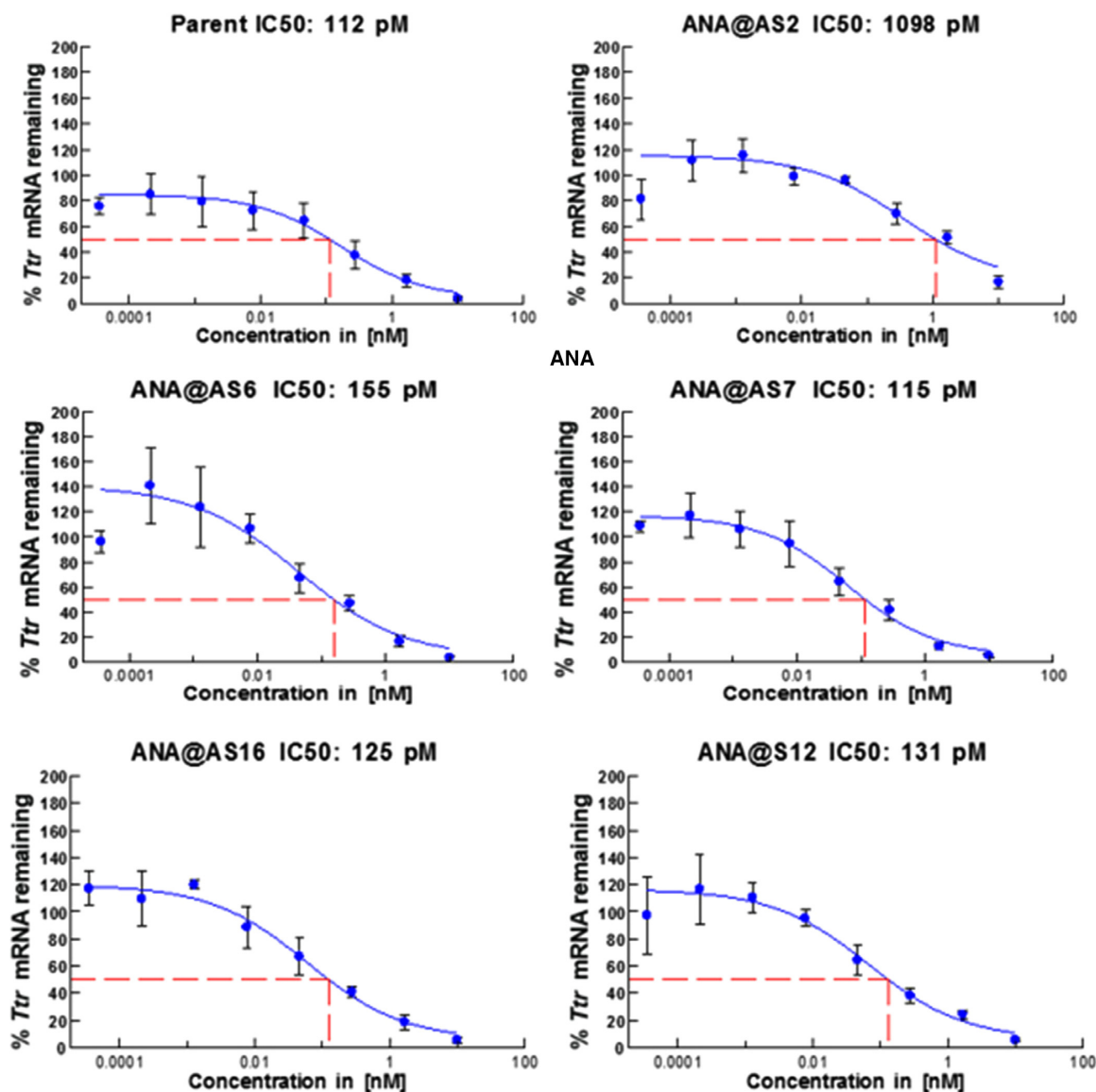
Figure 6. IC_{50} values of selected ANA-modified siRNAs in primary mouse hepatocytes. On y-axis % *Ttr* mRNA remaining relative to non-targeting siRNA-treated cells ($n = 4$, mean $\pm$ SD).

MID domain, and the lack of a 5′-monophosphate is known to impair RNAi activity (35,56–57). The RNAi activity was partially restored by installing a phosphate group chemically (Figure 2, AS1P). An ANA modification at position 2 of the antisense strand was also detrimental to RNAi activity, most likely owing to a structural incompatibility (see the 'Discussion' section for more details) as seen by the subtle and remarkable difference between 2′-F RNA and 2′-OMe RNA (14).

In the seed region of the siRNA antisense strand (nucleotides 2–8), the ANA modification was better accommodated. The modified duplexes with an ANA nucleotide at position 6 or 7 of the antisense strand had RNAi activity comparable to the parent duplex at 10 nM (Figure 2). In addition, the siRNA with ANA at position 16 of the antisense strand had activity comparable to the parent. How-

ever, none of the modified duplexes were more potent than the parent siRNA. Similar results were obtained at a lower concentration of 0.1 nM (Supplementary Figure S1). Single ANA modifications in the sense strand generally appear to lead to a slight loss in activity, although full dose response studies are needed to quantitate such small differences (Figure 3 and Supplementary Figure S2).

The position-dependent impact of the ANA modification on *in vitro* RNAi activity was also assessed in the absence of a transfecting agent, allowing free uptake of siRNAs (Figures 4 and 5; Supplementary Figures S3 and S4). Overall, the results obtained with free uptake correlates very well with the results when siRNAs were transfected. For instance, loss of activity was observed with ANA at position AS1 or AS2 while siRNAs containing ANA at position AS6 and AS7 maintained their activity.
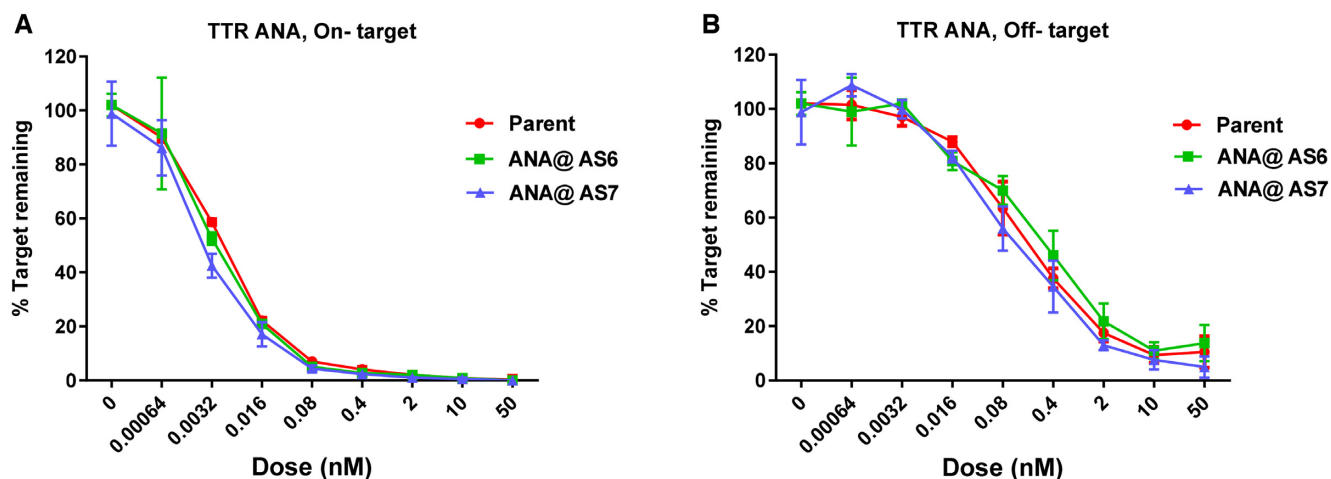
Figure 7. Analyses of on- and off-target effects of the ANA-modification in a luciferase reporter assay. Luciferase reporter plasmids were co-transfected with indicated siRNAs into COS-7 cells. The cells were harvested at 48 h after transfection. % Target remaining was calculated by dividing the ratio of Renilla/Firefly signal at each siRNA concentration by the ratio in the absence of siRNA.
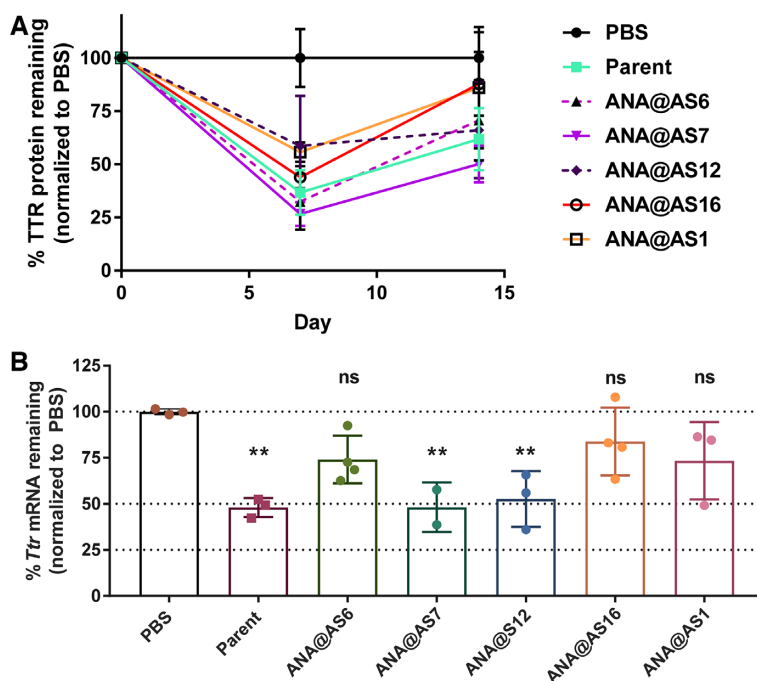

Figure 8. TTR protein and mRNA levels in C57BL/6 mice subcutaneously dosed with ANA-modified siRNAs. (**A**) Percent TTR protein in serum determined by ELISA relative to PBS-treated mice on days 7 and 14. Plotted are means ± SD ($n = 3$ animals per treatment cohort for PBS, parent, ANA@S12 and ANA@AS1 groups, $n = 4$ mice per treatment cohort for ANA@AS6 and ANA@AS16 groups, $n = 2$ for ANA@AS7). (**B**) Percent *Ttr* mRNA in the liver at day 14 relative to PBS-treated mice. Plotted are means ± SD (one-way ANOVA, **: $P < 0.005$, ns: non-statistically significant; $n = 3$ animals per treatment cohort for PBS, parent, ANA@S12 and ANA@AS1 groups, $n = 4$ mice per treatment cohort for ANA@AS6 and ANA@AS16 groups, $n = 2$ for ANA@AS7).

Based on the initial *in vitro* screening results, the IC_{50} values for several ANA-modified siRNAs were determined in primary mouse hepatocytes (Figure 6). The siRNA with an ANA at position 2 of the antisense strand was least potent (IC_{50} 1098 pM). The siRNA with ANA at position 7 of the sense strand had an IC_{50} value of 115 pM, which was within experimental error of the IC_{50} of the parent duplex (112 pM). The other ANA-modified siRNAs tested were also of similar potency.

Analysis of on-target and off-target activity in a luciferase reporter assay

Seed-mediated off-target activity has been reported to be a major driver of hepatotoxicity observed in rats for a subset of siRNAs (24). To reduce such off-target effects, thermodynamically duplex-destabilizing, acyclic modifications, such as glycol nucleic acid (GNA) have been incorporated into the seed regions of siRNA duplexes (24,27–32). GNA

mitigates seed-mediated off-target effects without reducing on-target potency. ANA is well tolerated in the seed region at positions 6 or 7 in the antisense strand and maintains on-target potency. This prompted us to evaluate the effect of ANA on potentially modulating the off-target activity using a luciferase reporter assay in which four regions that are matches to the seed region of the siRNA, but that are not complementary to the rest of the antisense strand, are cloned into the luciferase 3′-UTR region (29,45–46). The siRNAs with ANA at positions 6 and 7 of the antisense strand had on-target activity similar to the parent construct in this assay (Figure 7A), an observation consistent with earlier *in vitro* screening. The off-target activities for the parent duplex and for the ANA-modified duplexes were also the same within experimental error (Figure 7B). Thus, ANA neither reduces off-target activity nor enhances it. As ANA is not a thermodynamically destabilizing modification like GNA, this result is not surprising (vide infra).

Silencing of gene expression by ANA-modified GalNAc-siRNAs in mice

Selected siRNA duplexes were evaluated for their ability to silence the expression of the *Ttr* gene in mice. The animals were dosed at 1 mg/kg subcutaneously, with the control cohort receiving the 1 x PBS. Blood samples were collected just prior to the dosing and 7 and 14 days after dosing to evaluate circulating TTR protein levels in serum. At day 7, siRNAs with ANA at positions 6 or 7 of the antisense strand had potencies comparable to that of the parent duplex. However, at day 14, the siRNA with ANA at position 7 of the antisense strand had potency equivalent to the parent, whereas the siRNA with the ANA at position 6 was less potent (Figure 8A). The reason for this difference may be due to intrinsic metabolic stability differences, but this aspect needs further evaluation. The siRNA with the ANA modification at position 16 of the antisense strand was also significantly less active than the parent duplex (Figure 8A). This siRNA had activity comparable to the parent duplex *in vitro*, indicative of intrinsic differences between the *in vitro* and *in vivo* models. The siRNA with the sense strand modified with ANA at position 12 was slightly less active than the parent, but activity was maintained on day 14 (Figure 8A). The siRNA modified with ANA at the 5′ terminus of the antisense stand was not effective in mice (Figure 8A), possibly due to a lack of phosphorylation of the 5′-ANA by endogenous intracellular kinases. Improved RNAi activity *in vitro* for siRNA duplex carrying a chemically installed phosphate group at the 5′-end of antisense strand supported this hypothesis. However, an impact of the structural difference of ANA from RNA cannot be ruled out completely as an siRNA duplex with a phosphate group at the 5′-end was still less active than the parent duplex. In the *in vivo* experiments, the animals were sacrificed at day 14, and RNA from liver was extracted, followed by cDNA preparation and multiplexed RT-qPCR analysis to assess the *Ttr* mRNA levels (Figure 8B). The results were well aligned with those obtained from analysis of TTR protein in serum samples at day 14.
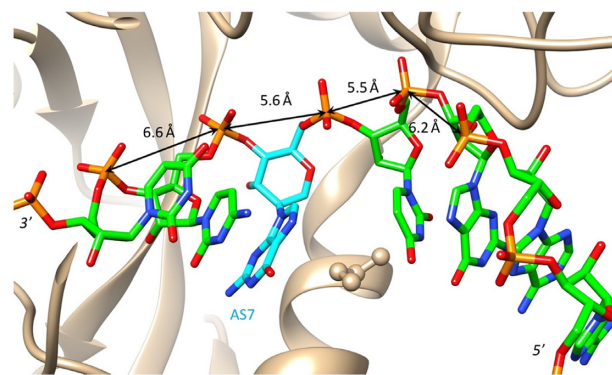

Figure 9. Model of the siRNA antisense strand with ANA-G at position 7 bound to Ago2. The ANA residue is highlighted with carbon atoms colored in cyan and selected intra-strand P-P distances are given in Å.

The conformation of ANA within an RNA strand

To gain insight into the effects of ANA substitutions, we built a model of an ANA-modified strand bound to Ago2. We used the crystal structure of the Ago2:miR-20a complex (48) as a starting point. The structure of the ANA residue incorporated in the RNA strand in place of G7 was taken from the crystal structure of an ANA:RNA decamer duplex (47). In the ANA:RNA duplex crystal structure, the intra-strand phosphate–phosphate distance for ANA residues is 5.53 Å on average; the distance for RNA residues was an average of 5.93 Å. The closer spacing between phosphates in ANA is due to the δ backbone torsion angle that averages 60° as a result of the chair conformation of the hexose. This angle is around 83° in the RNA strand of the hybrid duplex, a value identical to that in a canonical A-form RNA (58). The spacings between phosphates of residues 6 and 7 and 7 and 8 in miR-20a in the complex with Ago2 are shorter than the average distance between adjacent phosphates as a result of a pronounced kink at that site. Thus, an ANA nucleotide with an intrinsically short distance between the phosphate groups is well accommodated at position 7 (Figure 9).

Nuclease stability

To evaluate the effect of ANA on resistance of an oligonucleotide to exonuclease cleavage, one or two nucleotides at the 3′ or 5′ end of 5′-UsU(dT19)-3′ or 5′-(dT19)UsU-3′, respectively, where 's' indicates a phosphorothioate linkage in the otherwise phosphodiester-linked oligonucleotide. Stabilities of the ANA-modified strands were compared to the strands with one or two uridines at the appropriate terminus. Oligonucleotides modified at the 3′ end were incubated with snake venom phosphodiesterase (SVPD), a 3′-exonuclease and the degradation of full-length oligonucleotide was monitored using ion-exchange HPLC. Oligonucleotides with two uridines or an ANA had similar stability against SVPD and thus comparable half-lives. The oligonucleotide with two ANA residues had 2-fold longer half-life (Figure 10A).

The 5′-modified oligonucleotides were incubated with phosphodiesterase II (PDEII), a 5′-specific exonuclease.
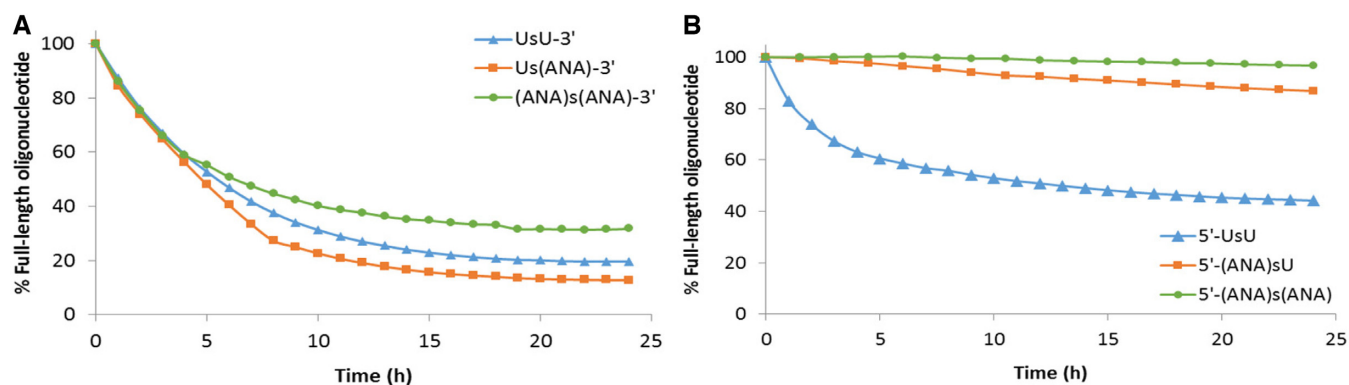
Figure 10. Stability of oligonucleotides carrying ANA modifications in the presence of (**A**) SVPD and (**B**) PDEII. Oligonucleotides tested contain one or two nucleotides at the 3′ or 5′ end of 5′-UsU(dT19)-3′ or 5′-(dT19)UsU-3′, respectively, where 's' indicates a phosphorothioate linkage in the otherwise phosphodiester-linked oligonucleotides.

The oligonucleotide carrying a single ANA modification at the 5′ end was considerably more stable compared to the oligonucleotide carrying uridine. Addition of a second ANA modification at the 5′ end rendered the oligonucleotide inert for a duration of 24 h under the tested conditions (Figure 10B). When an ANA dimer was superimposed on the two 5′-terminal dTs present in the crystal structure of oligo-dT bound to the 5′-exoribonuclease Xrn1 (51), differences were observed in inter-phosphate spacing (shorter for ANA) and phosphate orientation; the increased bulk of the hexose sugar compared to 2′-deoxyribose is also apparent (Figure 11A). Conversely, comparison between the crystal structure of DNA bound to DNA polymerase I Klenow fragment 3′-exonuclease (52) and models of RNA and ANA bound to the same active site reveals only very minor deviations between the orientations of the scissile phosphate group in the three species (Figure 11B). Moreover, the models support the conclusion that additional sugar hydroxyl groups in the RNA and ANA dimers relative to DNA can be accommodated without generating clashes with exonuclease active site residues.

DISCUSSION

Altritol nucleic acids (ANA) have a hexopyranose ring system with a preorganized structure similar to the conformation of an *N*-type furanose sugar, and the presence of the hydroxyl group at the 3′-position contributes to duplex stabilization. The RNA-like A-type geometry of ANA makes it a candidate for incorporation into siRNAs and ANA-modified siRNAs have been evaluated showing therapeutic promise (28,42–44), however the ANA modification had not been tested in the context of fully modified nucleotides or in GalNAc-siRNA conjugates. Here we evaluated *in vitro* and *in vivo* gene silencing activity of siRNA duplexes modified with ANA, 2′-F RNA and 2′-OMe RNA nucleotides and conjugated to GalNAc. We also evaluated how ANA nucleotides protected oligonucleotides from nucleolytic degradation.

Placement of a single ANA nucleotide along the siRNA antisense strand (AS) manifested *in vitro* activities that were comparable to the performance of the parent duplex for
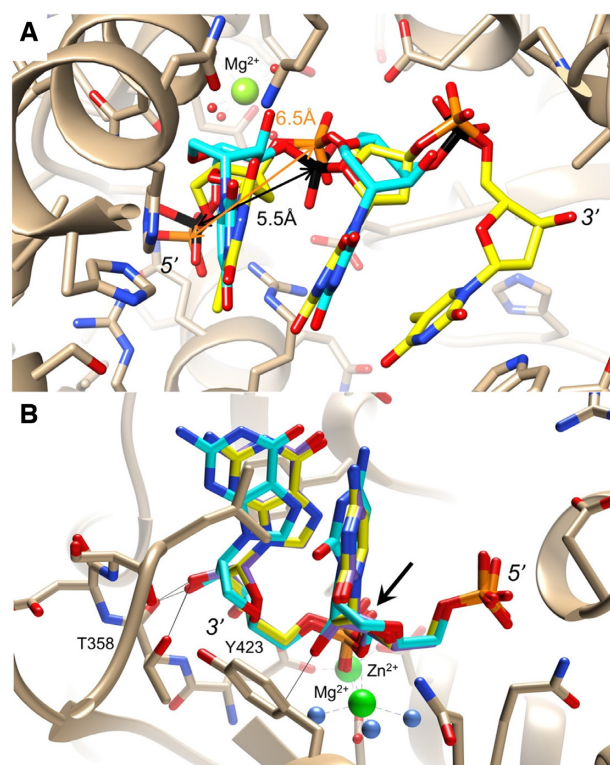

Figure 11. (**A**) Active site view of Xrn1 5′-exoribonuclease bound to 5′-P-dTdTdT-3′, where P is a phosphate (phosphorus and carbon atoms colored in orange and yellow, respectively) as observed in the crystal structure of the complex (51). The superimposed ANA dimer (phosphorus and carbon atoms colored in black and cyan, respectively) reveals deviations in phosphate-phosphate spacings between ANA and DNA (black and orange arrows, respectively) and in phosphate orientations relative to the Mg^{2+} ion (green sphere). (**B**) Active site view of Klenow fragment 3′-exonuclease bound to 3′-dGdC-*P*-5′, where P is a phosphate (phosphorus and carbon atoms colored in orange and yellow, respectively) as observed in the crystal structure of the complex (52). The superimposed complex models with RNA dimer (carbon atoms colored in purple) and ANA dimer (carbon atoms colored in cyan) reveal similar orientations of the scissile phosphate (marked by an arrow) in the three dimers relative to metal ions A and B (green spheres; water molecules are smaller spheres colored in light blue). The closest distance between RNA/ANA 2′-OH(C) and Tyr-423 is ca. 3 Å and distances between RNA/ANA 2′-OH(G) and Thr-358 (O, Oγ) range from 2.2 to 2.8 Å.
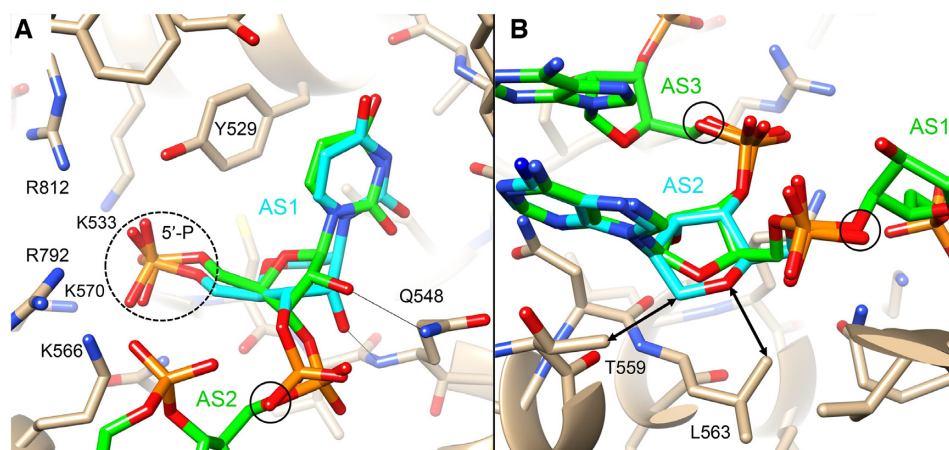
Figure 12. Models of Ago2 interactions with siRNA guide strand nucleotides (**A**) AS1 replaced by an ANA residue, and (**B**) AS2 replaced by an ANA residue. An ANA nucleotide (5′,3′-diphosphate) excised from the crystal structure of an ANA:RNA hybrid duplex (PDB ID: 3OK2) (47) was superimposed on either the AS1 or AS2 nucleotide of miR-20a in complex with Ago2 (PDB ID: 4F3T) (48) using the match option in the program UCSF Chimera (49). To improve the fit, selected backbone torsion angles and the glycosidic angle of the ANA nucleotide were adjusted, without, however, altering the synclinal or antiperiplanar angle ranges. ANA and RNA carbon atoms are colored in cyan and green, respectively, H-bonds are drawn with thin solid lines (panel A), potential clashes are indicated by arrows (panel B), and near overlaps of 5′-/3′-oxygen atoms and the 5′-phosphate group are highlighted by solid and dashed circles, respectively.

strands with ANA at positions AS6, AS7 or AS16. Further evaluation of ANA-modified duplexes *in vivo* showed that ANA at AS7 retains favorable potency, whereas siRNAs with ANA at either position AS6 or AS16 displayed lower activities compared to those seen *in vitro*. The intrinsically shorter phosphate–phosphate spacing in an oligo-ANA backbone compared to RNA appears to render the modification ideal for insertion at position AS7 that is characterized by a kink in the crystal structure of an miRNA:Ago2 complex (48). Indeed, molecular modeling supports this view, whereby replacement of ribonucleotide AS7 by ANA reveals a seamless fit at the site of the kink (Figure 9). Although ANA features the same 5-atom linker (O5′, C5′, C4′, C3′, O3′) between phosphate groups as RNA, the chair conformation of the altritol sugar with an ideal δ torsion angle of 60° results in shorter phosphate–phosphate spacings relative to RNA (δ ≅ 83°, A-form). We previously investigated the effects of glycol nucleic acid (GNA) modification in the guide and passenger strands on siRNA activity (25). GNA features a 4-atom linker that also leads to tighter spacing of adjacent phosphates relative to RNA, and an siRNA with (*R*)-GNA incorporated at AS7 displayed favorable potency compared to the parent duplex. Therefore, two xeno nucleic acids, one based on a hexose sugar and the other on an acyclic framework, offer similar benefits in terms of enhanced siRNA activity by mimicking a particularly short phosphate-phosphate distance at a kink in the seed region of the guide strand loaded into Ago2. GNA nucleotides when incorporated at position 6 or 7 in the seed region of the antisense strand also reduced the off-target events. However, the luciferase reporter assay indicated that ANA at position 6 or 7 in the seed region of the antisense strand of the tested siRNA against TTR did not affect its off-target activity. While promising, additional siRNA sequences need to be evaluated in this assay to make a generalizable conclusion about the effects of ANA on undesired off-target activity of siRNAs. As the mitigation of off-target

effects is related to the thermal stability of the seed region with potential off-target mRNAs, GNA-based xeno nucleic acid seemed to perform better as ANA is not a thermally destabilizing modification (40).

It is noteworthy that the activity of guide siRNA with ANA at AS1 is only slightly reduced relative to the parent RNA (Figure 2). Conversely, ANA at AS2 results in the most significant loss in activity compared to any position in both the guide and passenger strands (Figures 2 and 3). Unlike the ribose in RNA, the altritol sugar cannot adopt a different pucker, and its ANA-hydroxyl group is locked in the axial orientation. However, the ribonucleotide at the 5′-terminal position of the guide strand (AS1) and docked to the Ago2 MID domain adopts the atypical C2′-*endo* and C1′-*exo* puckers (14). Thus, the ANA-hydroxyl group is in an equatorial orientation and engaged in a H-bond with the side chain of Q548 (Figure 12A). Despite these differences in sugar constitution and conformation, ANA-U can be overlaid onto the first nucleotide of the guide strand such that base stacking on Y529, 5′-phosphate interactions with various lysine and arginine side chains as well as the proper geometry of the connection to the AS2 nucleotide are maintained (Figure 12A). Interestingly, the model suggests that the ANA -OH group can engage in a H-bond with the main chain amino group of Q548.

Moving to the AS2 position and overlaying ANA-A on the ribonucleotide there at first leads to a similar impression, i.e. the orientations of the 5′- and 3′-phosphate groups and the nucleobase match very well. However, the altritol sugar is bulkier than ribose and a distance of 3.3 Å between the C6′ sugar carbon and the methyl group of T559 as well as a distance of 3.5 Å between O4′ and the side chain of L563 in the model indicate potential clashes (Figure 12B). Avoiding these would require movement of the AS2 nucleotide, the α-helix that packs against the second nucleotide of the guide strand, or both. However, it is well known that 2′-*O*-methyl modification of the nucleotide at

AS2 is not tolerated (14), as it causes short contacts with amino acids from an adjacent α-helical turn. This indicates that the α-helix does not go out of the way to accommodate the methoxy substituent and that the 5′- and 3′-phosphates of AS2 are firmly held in place by interactions with Ago2 side chains. The most likely culprit behind the significantly reduced potency of guide siRNAs with ANA at AS2 is therefore a steric conflict between altritol sugar atoms and Ago2 MID domain residues (Figure 12B). Interestingly, the observed high nuclease resistance of RNAs with dual ANA modification at the 5′-end is most likely also a consequence of steric conflicts in addition to the tighter phosphate–phosphate spacing in ANA (Figure 11).

In summary, we have shown that siRNAs modified with a single altritol six-membered sugar ring induce efficient gene silencing both *in vitro* and *in vivo* when judiciously introduced within the siRNA duplex. Specifically, the ANA modification was best accommodated at position 7 of the antisense strand. Previous crystallographic data for an ANA:RNA hybrid revealed that the average distance between the 5′- and 3′-phosphates of an ANA residue is shorter than the average distance between phosphates in RNA. An ANA residue can thus sufficiently mimic a ribonucleotide at position 7 of the antisense strand bound to Ago2, a site at which a kink in the siRNA antisense strand results in local contraction of phosphate–phosphate distances. Oligonucleotides with ANA at the 5′ end were considerably more resistant to degradation with the 5′-exonuclease PDEII than natural RNA counterparts. However, this significant gain in stability was not observed in assays testing resistance against degradation by SVPD, a 3′-exonuclease. A model of an oligonucleotide with two ANA-uridines at the 5′ end bound to a 5′-exoribonuclease indicates that steric bulk and altered phosphate–phosphate spacing relative to RNA likely underlie the nuclease resistance. By comparison, our modeling studies suggest that an ANA dimer can be accommodated at the active site of a 3′-exonuclease without clashes. Further evaluation of siRNAs carrying strategically placed ANA nucleotides, as investigated in the current study, against different gene targets is warranted.

SUPPLEMENTARY DATA

Supplementary Data are available at NAR Online.

ACKNOWLEDGEMENTS

FUNDING

REFERENCES

1. Adams,D., Gonzalez-Duarte,A., O'Riordan,W.D., Yang,C.-C., Ueda,M., Kristen,A.V, Tournev,I., Schmidt,H.H., Coelho,T., Berk,J.L. *et al.* (2018) Patisiran, an RNAi therapeutic, for hereditary transthyretin amyloidosis. *N. Engl. J. Med.*, **379**, 11–21.
2. Chan,A., Liebow,A., Yasuda,M., Gan,L., Racie,T., Maier,M., Kuchimanchi,S., Foster,D., Milstein,S., Charisse,K. *et al.* (2015) Preclinical development of a subcutaneous ALAS1 RNAi therapeutic for treatment of hepatic porphyrias using circulating RNA quantification. *Mol. Ther. Nucleic Acids*, **4**, e263–e263.
3. Sardh,E., Harper,P., Balwani,M., Stein,P., Rees,D., Bissell,D.M., Desnick,R., Parker,C., Phillips,J., Bonkovsky,H.L. *et al.* (2019) Phase 1 trial of an RNA interference therapy for acute intermittent porphyria. *N. Engl. J. Med.*, **380**, 549–558.
4. Rajeev,K.G. and Manoharan,M. (2019) CHAPTER 11 liver-targeted RNAi therapeutics: principles and applications. In: Agrawal,S and Gait,MJ (eds). *Advances in Nucleic Acid Therapeutics*. The Royal Society of Chemistry, pp. 233–265.
5. Shen,X. and Corey,D.R. (2018) Chemistry, mechanism and clinical status of antisense oligonucleotides and duplex RNAs. *Nucleic Acids Res.*, **46**, 1584–1600.
6. Akinc,A., Maier,M.A., Manoharan,M., Fitzgerald,K., Jayaraman,M., Barros,S., Ansell,S., Du,X., Hope,M.J., Madden,T.D. *et al.* (2019) The Onpattro story and the clinical translation of nanomedicines containing nucleic acid-based drugs. *Nat. Nanotechnol.*, **14**, 1084–1087.
7. Chakraborty,C., Sharma,A.R., Sharma,G., Doss,C.G.P. and Lee,S.-S. (2017) Therapeutic miRNA and siRNA: moving from bench to clinic as next generation medicine. *Mol. Ther. Nucleic Acids*, **8**, 132–143.
8. Elbashir,S.M., Harborth,J., Lendeckel,W., Yalcin,A., Weber,K. and Tuschl,T. (2001) Duplexes of 21-nucleotide RNAs mediate RNA interference in cultured mammalian cells. *Nature*, **411**, 494–498.
9. Caplen,N.J., Parrish,S., Imani,F., Fire,A. and Morgan,R.A. (2001) Specific inhibition of gene expression by small double-stranded RNAs in invertebrate and vertebrate systems. *Proc. Natl. Acad. Sci. U.S.A.*, **98**, 9742–9747.
10. Chiu,Y.-L. and Rana,T.M. (2003) siRNA function in RNAi: a chemical modification analysis. *RNA*, **9**, 1034–1048.
11. Braasch,D.A., Jensen,S., Liu,Y., Kaur,K., Arar,K., White,M.A. and Corey,D.R. (2003) RNA interference in mammalian cells by chemically-modified RNA. *Biochemistry*, **42**, 7967–7975.
12. Allerson,C.R., Sioufi,N., Jarres,R., Prakash,T.P., Naik,N., Berdeja,A., Wanders,L., Griffey,R.H., Swayze,E.E. and Bhat,B. (2005) Fully 2′-modified oligonucleotide duplexes with improved in vitro potency and stability compared to unmodified small interfering RNA. *J. Med. Chem.*, **48**, 901–904.
13. Manoharan,M. (2004) RNA interference and chemically modified small interfering RNAs. *Curr. Opin. Chem. Biol.*, **8**, 570–579.
14. Egli,M. and Manoharan,M. (2019) Re-engineering RNA molecules into therapeutic agents. *Acc. Chem. Res.*, **52**, 1036–1047.
15. Deleavey,G.F., Watts,J.K., Alain,T., Robert,F., Kalota,A., Aishwarya,V., Pelletier,J., Gewirtz,A.M., Sonenberg,N. and Damha,M.J. (2010) Synergistic effects between analogs of DNA and RNA improve the potency of siRNA-mediated gene silencing. *Nucleic Acids Res.*, **38**, 4547–4557.
16. Manoharan,M., Akinc,A., Pandey,R.K., Qin,J., Hadwiger,P., John,M., Mills,K., Charisse,K., Maier,M.A., Nechev,L. *et al.* (2011) Unique gene-silencing and structural properties of 2′-fluoro-modified siRNAs. *Angew. Chem. Int. Ed. Engl.*, **50**, 2284–2288.
17. Hassler,M.R., Turanov,A.A., Alterman,J.F., Haraszti,R.A., Coles,A.H., Osborn,M.F., Echeverria,D., Nikan,M., Salomon,W.E., Roux,L. *et al.* (2018) Comparison of partially and fully chemically-modified siRNA in conjugate-mediated delivery in vivo. *Nucleic Acids Res.*, **46**, 2185–2196.
18. Janas,M.M., Zlatev,I., Liu,J., Jiang,Y., Barros,S.A., Sutherland,J.E., Davis,W.P., Liu,J., Brown,C.R., Liu,X. *et al.* (2019) Safety evaluation of 2′-deoxy-2′-fluoro nucleotides in GalNAc-siRNA conjugates. *Nucleic Acids Res.*, **47**, 3306–3320.
19. Behlke,M.A. (2008) Chemical modification of siRNAs for in vivo use. *Oligonucleotides*, **18**, 305–320.
20. Morrissey,D.V, Lockridge,J.A., Shaw,L., Blanchard,K., Jensen,K., Breen,W., Hartsough,K., Machemer,L., Radka,S., Jadhav,V. *et al.*

(2005) Potent and persistent in vivo anti-HBV activity of chemically modified siRNAs. *Nat. Biotechnol.*, **23**, 1002–1007.

21. Morrissey,D.V, Blanchard,K., Shaw,L., Jensen,K., Lockridge,J.A., Dickinson,B., McSwiggen,J.A., Vargeese,C., Bowman,K., Shaffer,C.S. *et al.* (2005) Activity of stabilized short interfering RNA in a mouse model of hepatitis B virus replication. *Hepatology*, **41**, 1349–1356.

22. Setten,R.L., Rossi,J.J. and Han,S. (2019) The current state and future directions of RNAi-based therapeutics. *Nat. Rev. Drug Discov.*, **18**, 421–446.

23. Kumar,P., Parmar,R.G., Brown,C.R., Willoughby,J.L.S., Foster,D., Babu,R.I., Schofield,S., Jadhav,V., Charisse,K., Nair,J.K. *et al.* (2019) 5′-Morpholino modification of the sense strand of an siRNA makes it a more effective passenger. *Chem. Commun.*, **55**, 5139–5142.

24. Janas,M.M., Schlegel,M.K., Harbison,C.E., Yilmaz,V.O., Jiang,Y., Parmar,R., Zlatev,I., Castoreno,A., Xu,H., Shulga-Morskaya,S. *et al.* (2018) Selection of GalNAc-conjugated siRNAs with limited off-target-driven rat hepatotoxicity. *Nat. Commun.*, **9**, 723.

25. Schlegel,M.K., Foster,D.J., Kel'in,A.V, Zlatev,I., Bisbe,A., Jayaraman,M., Lackey,J.G., Rajeev,K.G., Charissé,K., Harp,J. *et al.* (2017) Chirality dependent potency enhancement and structural impact of glycol nucleic acid modification on siRNA. *J. Am. Chem. Soc.*, **139**, 8537–8546.

26. Malek-Adamian,E., Guenther,D.C., Matsuda,S., Martínez-Montero,S., Zlatev,I., Harp,J., Burai Patrascu,M., Foster,D.J., Fakhoury,J., Perkins,L. *et al.* (2017) 4′-C-Methoxy-2′-deoxy-2′-fluoro modified ribonucleotides improve metabolic stability and elicit efficient RNAi-mediated gene silencing. *J. Am. Chem. Soc.*, **139**, 14542–14555.

27. Bramsen,J.B., Pakula,M.M., Hansen,T.B., Bus,C., Langkjær,N., Odadzic,D., Smicius,R., Wengel,S.L., Chattopadhyaya,J., Engels,J.W. *et al.* (2010) A screen of chemical modifications identifies position-specific modification by UNA to most potently reduce siRNA off-target effects. *Nucleic Acids Res.*, **38**, 5761–5773.

28. Bramsen,J.B., Laursen,M.B., Nielsen,A.F., Hansen,T.B., Bus,C., Langkjaer,N., Babu,B.R., Højland,T., Abramov,M., Van Aerschot,A. *et al.* (2009) A large-scale chemical modification screen identifies design rules to generate siRNAs with high activity, high stability and low toxicity. *Nucleic Acids Res.*, **37**, 2867–2881.

29. Vaish,N., Chen,F., Seth,S., Fosnaugh,K., Liu,Y., Adami,R., Brown,T., Chen,Y., Harvie,P., Johns,R. *et al.* (2011) Improved specificity of gene silencing by siRNAs containing unlocked nucleobase analogs. *Nucleic Acids Res.*, **39**, 1823–1832.

30. Lee,H.-S., Seok,H., Lee,D.H., Ham,J., Lee,W., Youm,E.M., Yoo,J.S., Lee,Y.-S., Jang,E.-S. and Chi,S.W. (2015) Abasic pivot substitution harnesses target specificity of RNA interference. *Nat. Commun.*, **6**, 10154.

31. Seok,H., Jang,E.-S. and Chi,S.W. (2016) Rationally designed siRNAs without miRNA-like off-target repression. *BMB Rep.*, **49**, 135–136.

32. Mook,O., Vreijling,J., Wengel,S.L., Wengel,J., Zhou,C., Chattopadhyaya,J., Baas,F. and Fluiter,K. (2010) In vivo efficacy and off-target effects of locked nucleic acid (LNA) and unlocked nucleic acid (UNA) modified siRNA and small internally segmented interfering RNA (sisiRNA) in mice bearing human tumor xenografts. *Artif. DNA. PNA XNA*, **1**, 36–44.

33. Elkayam,E., Parmar,R., Brown,C.R., Willoughby,J.L., Theile,C.S., Manoharan,M. and Joshua-Tor,L. (2016) siRNA carrying an (E)-vinylphosphonate moiety at the 5′ end of the guide strand augments gene silencing by enhanced binding to human Argonaute-2. *Nucleic Acids Res.*, **45**, 3528–3536.

34. Parmar,R., Willoughby,J.L.S., Liu,J., Foster,D.J., Brigham,B., Theile,C.S., Charisse,K., Akinc,A., Guidry,E., Pei,Y. *et al.* (2016) 5′-(E)-Vinylphosphonate: a stable phosphate mimic can improve the RNAi activity of siRNA–GalNAc conjugates. *ChemBioChem*, **17**, 985–989.

35. Parmar,R.G., Brown,C.R., Matsuda,S., Willoughby,J.L.S., Theile,C.S., Charissé,K., Foster,D.J., Zlatev,I., Jadhav,V., Maier,M.A. *et al.* (2018) Facile synthesis, geometry, and 2′-substituent-dependent in vivo activity of 5′-(E)- and 5′-(Z)-Vinylphosphonate-Modified siRNA conjugates. *J. Med. Chem.*, **61**, 734–744.

36. Lima,W.F., Prakash,T.P., Murray,H.M., Kinberger,G.A., Li,W., Chappell,A.E., Li,C.S., Murray,S.F., Gaus,H., Seth,P.P. *et al.* (2012)

37. Yu,D., Pendergraff,H., Liu,J., Kordasiewicz,H.B., Cleveland,D.W., Swayze,E.E., Lima,W.F., Crooke,S.T., Prakash,T.P. and Corey,D.R. (2012) Single-stranded RNAs use RNAi to potently and allele-selectively inhibit mutant huntingtin expression. *Cell*, **150**, 895–908.

38. Prakash,T.P., Lima,W.F., Murray,H.M., Li,W., Kinberger,G.A., Chappell,A.E., Gaus,H., Seth,P.P., Bhat,B., Crooke,S.T. *et al.* (2015) Identification of metabolically stable 5′-phosphate analogs that support single-stranded siRNA activity. *Nucleic Acids Res.*, **43**, 2993–3011.

39. Prakash,T.P., Lima,W.F., Murray,H.M., Elbashir,S., Cantley,W., Foster,D., Jayaraman,M., Chappell,A.E., Manoharan,M., Swayze,E.E. *et al.* (2013) Lipid nanoparticles improve activity of single-stranded siRNA and gapmer antisense oligonucleotides in animals. *ACS Chem. Biol.*, **8**, 1402–1406.

40. Allart,B., Khan,K., Rosemeyer,H., Schepers,G., Hendrix,C., Rothenbacher,K., Seela,F., Van Aerschot,A. and Herdewijn,P. (1999) D-Altritol Nucleic Acids (ANA): hybridisation properties, stability, and initial structural analysis. *Chem. A Eur. J.*, **5**, 2424–2431.

41. Allart,B., Busson,R., Rozenski,J., Van Aerschot,A. and Herdewijn,P. (1999) Synthesis of protected D-altritol nucleosides as building blocks for oligonucleotide synthesis. *Tetrahedron*, **55**, 6527–6546.

42. Fisher,M., Abramov,M., Van Aerschot,A., Xu,D., Juliano,R.L. and Herdewijn,P. (2007) Inhibition of MDR1 expression with altritol-modified siRNAs. *Nucleic Acids Res.*, **35**, 1064–1074.

43. Fisher,M., Abramov,M., Van Aerschot,A., Rozenski,J., Dixit,V., Juliano,R.L. and Herdewijn,P. (2009) Biological effects of hexitol and altritol-modified siRNAs targeting B-Raf. *Eur. J. Pharmacol.*, **606**, 38–44.

44. Hean,J., Crowther,C., Ely,A., Ul Islam,R., Barichievy,S., Bloom,K., Weinberg,M.S., van Otterlo,W. Al, de Koning,C.B., Salazar,F. *et al.* (2010) Inhibition of hepatitis B virus replication in vivo using lipoplexes containing altritol-modified antiviral siRNAs. *Artif. DNA. PNA XNA*, **1**, 17–26.

45. Ui-Tei,K., Naito,Y., Nishi,K., Juni,A. and Saigo,K. (2008) Thermodynamic stability and Watson-Crick base pairing in the seed duplex are major determinants of the efficiency of the siRNA-based off-target effect. *Nucleic Acids Res.*, **36**, 7100–7109.

46. Doench,J.G., Petersen,C.P. and Sharp,P.A. (2003) siRNAs can function as miRNAs. *Genes Dev.*, **17**, 438–442.

47. Ovaere,M., Sponer,J., Sponer,J.E., Herdewijn,P. and Van Meervelt,L. (2012) How does hydroxyl introduction influence the double helical structure: the stabilization of an altritol nucleic acid:ribonucleic acid duplex. *Nucleic Acids Res.*, **40**, 7573–7583.

48. Elkayam,E., Kuhn,C.-D., Tocilj,A., Haase,A.D., Greene,E.M., Hannon,G.J. and Joshua-Tor,L. (2012) The structure of human argonaute-2 in complex with miR-20a. *Cell*, **150**, 100–110.

49. Pettersen,E.F., Goddard,T.D., Huang,C.C., Couch,G.S., Greenblatt,D.M., Meng,E.C. and Ferrin,T.E. (2004) UCSF Chimera—a visualization system for exploratory research and analysis. *J. Comput. Chem.*, **25**, 1605–1612.

50. Case,D.A., Babin,V., Berryman,J.T., Betz,R.M., Cai,Q., Cerutti,D.S., Cheatham,T.E. III, Darden,T.A., Duke,R.E., Gohlke,H. *et al.* (2014) *AMBER 14.* https://ambermd.org/doc12/Amber14.pdf.

51. Jinek,M., Coyle,S.M. and Doudna,J.A. (2011) Coupled 5′ nucleotide recognition and processivity in Xrn1-mediated mRNA decay. *Mol. Cell*, **41**, 600–608.

52. Brautigam,C.A. and Steitz,T.A. (1998) Structural principles for the inhibition of the 3′-5′ exonuclease activity of Escherichia coli DNA polymerase I by phosphorothioates 11Edited by R. Huber. *J. Mol. Biol.*, **277**, 363–377.

53. Matsuda,S., Keiser,K., Nair,J.K., Charisse,K., Manoharan,R.M., Kretschmer,P., Peng,C.G., Kel'in,A.V., Kandasamy,P., Willoughby,J.L.S. *et al.* (2015) siRNA conjugates carrying sequentially assembled trivalent N-Acetylgalactosamine linked through nucleosides elicit robust gene silencing in vivo in hepatocytes. *ACS Chem. Biol.*, **10**, 1181–1187.

54. Nair,J.K., Willoughby,J.L.S., Chan,A., Charisse,K., Alam,M.R., Wang,Q., Hoekstra,M., Kandasamy,P., Kel'in,A.V, Milstein,S. *et al.* (2014) Multivalent N-Acetylgalactosamine-conjugated siRNA localizes in hepatocytes and elicits robust RNAi-mediated gene silencing. *J. Am. Chem. Soc.*, **136**, 16958–16961.

55. Rajeev,K.G., Nair,J.K., Jayaraman,M., Charisse,K., Taneja,N., O'Shea,J., Willoughby,J.L.S., Yucius,K., Nguyen,T., Shulga-Morskaya,S. *et al.* (2015) Hepatocyte-specific delivery of siRNAs conjugated to novel Non-nucleosidic trivalent N-Acetylgalactosamine elicits robust gene silencing in vivo. *ChemBioChem*, **16**, 903–908.

56. Schirle,N.T. and MacRae,I.J. (2012) The crystal structure of human Argonaute2. *Science*, **336**, 1037–1040.

57. Wang,Y., Juranek,S., Li,H., Sheng,G., Wardle,G.S., Tuschl,T. and Patel,D.J. (2009) Nucleation, propagation and cleavage of target RNAs in Ago silencing complexes. *Nature*, **461**, 754–761.

58. Saenger,W. (1984) In: Neidle,S (ed). *Principles of Nucleic Acid Structure*. Springer-Verlag, NY, p. 556.